A partial distal forelimb of a woolly rhino (Coelodonta antiquitatis) from Wadersloh (Westphalia, Germany) and insights from bone compactness

Article *in* Geologie und Palaeontologie in Westfalen · March 2021

CITATIONS
0

READS
29

2 authors, including:

Rico Schellhorn
University of Bonn
35 PUBLICATIONS **228** CITATIONS

SEE PROFILE

Geologie und Paläontologie in Westfalen (online first): 1-21

A partial distal forelimb of a woolly rhino (*Coelodonta antiquitatis*) from Wadersloh (Westphalia, Germany) and insights from bone compactness

Rico Schellhorn & Manfred Schlösser

Rico Schellhorn
Institut für Geowissenschaften
Rheinische Friedrich-Wilhelms-Universität Bonn
Nussallee 8
53115 Bonn

Manfred Schlösser
LWL-Museum für Naturkunde
Westfälisches Landesmuseum mit Planetarium
Sentruper Straße 285
48161 Münster

Corresponding author:
rico.schellhorn@uni-bonn.de

Manuscript
Recieved: 16.12.2020
Accepted: 01.03.2021
Available online: 29.03.2021

Abstract

During the late Pleistocene, as an important faunal element, the woolly rhinoceros (*Coelodonta antiquitatis*) was adapted to the cold glacial climates of Eurasia. Such adaptations were a woolly fur against low temperatures and a head posture to feed on low vegetation like herbs. Here we describe the bones of a partial lower forelimb of a woolly rhino. The bones were found in a gravel pit and are according to their dimensions belonging to one individual. Associated postcranial bones are often scarce, and even more often phalanges and carpal bones are missing. This material consists of radius, three carpal bones, three metacarpal bones, and two phalanges of a left forelimb. From the Wadersloh area rhino teeth are known and this finding is the most complete postcranial material of one individual for this region. The bones are scanned by micro-computed tomography and the bone compactness values are calculated for the radius and the metacarpals. These values are compared to data of an extant pygmy hippo and Miocene rhinoceroses from Sandelzhausen to analyze ecological adaptations. As a result, the values of the aquatic pygmy hippo are similar to the values of the undoubtedly terrestrial woolly rhino. Therefore, bone compactness might not be the best tool to state about possible semiaquatic adaptations in fossil rhinos. The high compactness might be due to the behavior of wallowing in rhinos and/or due to the large body weight.

Keywords: carpals, metacarpals, Pleistocene, Rhinocerotidae, ecological adaptation

Kurzfassung

Das Wollnashorn (*Coelodonta antiquitatis*) stellt ein wichtiges Element der jungpleistozänen Fauna Eurasiens dar. Mit einem dichten Fell ist es an kalte Klimate angepasst und ernährte sich mit einer gesenkten Kopfhaltung von flachwachsenden Pflanzen wie zum Beispiel Kräutern. In dieser Studie werden die Knochen einer unvollständig erhaltenen Vorderextremität eines Wollnashorns beschrieben. Die Knochen wurden zusammen in einer Kiesgrube gefunden und aufgrund entsprechender Abmessungen wird davon ausgegangen, dass die Reste zu einem Individuum gehören. Zusammengehörige Knochen des postcranialen Skelettes sind selten und gerade Handwurzelknochen und Fingerknochen fehlen oft. Das hier beschriebene Material besteht aus einem Radius (Speiche), drei Handwurzelknochen, drei Mittelhandknochen und zwei Phalangen (Fingerknochen) einer linken Vorderextremität. Von Wadersloh sind bereits Wollnashornzähne bekannt und dieser Fund stellt das vollständigste zusammenhängende postcraniale Material eines Wollnashorns dieser Region dar. Aufgrund der Tatsache, dass die Knochen zu einem Individuum gehören, wurden Radius und Metacarpalia mittels Mikrocomputertomographie gescannt und bezüglich der Verteilung von kompaktem zu spongiösem Knochen untersucht. Um Rückschlüsse auf ökologische Anpassungen ziehen zu können, wurden die gewonnenen Werte mit den Werten eines heutigen Zwergflusspferdes und der Nashörner der miozänen Fundstelle Sandelzhausen verglichen. Dabei ähneln die Werte des aquatischen Zwergflusspferdes denen des unzweifelhaft terrestrischen Wollnashorns sehr. Infolge dieser Ergebnisse ist die Untersuchung der Knochenkompaktheit nicht das beste Werkzeug um eine mögliche Anpassung an aquatische Lebensräume ausgestorbener Nashörner zu untersuchen. Die hohe Kompaktheit der Nashornknochen könnte daher rühren, dass Nashörner sich oft suhlen und/oder sie ist durch das hohe Körpergewicht bedingt.

Schlagwörter: Handwurzelknochen, Mittelhandknochen, Pleistozän, Rhinocerotidae, ökologische Anpassung

Introduction

Coelodonta antiquitatis (Blumenbach, 1799) – the woolly rhinoceros – belongs to the large mammal fauna of the late Pleistocene of Eurasia (Kahlke & Lacombat 2008). Together with the woolly mammoth (*Mammuthus primigenius*) both taxa are characteristic species of the cold Pleistocene periods (Koenigswald 2007). The genus *Coelodonta* originated in the middle Pliocene in Tibet with the basal species *C. thibetana* (Deng et al. 2011). Other species are *C. nihowanensis* from the early Pleistocene of northern China, *C. tologoijensis* from the middle Pleistocene of eastern Siberia and western Europe, and the most derived species *C. antiquitatis* from the late Pleistocene of northern Eurasia (Deng et al. 2011). The findings of the woolly rhinoceros in North Rhine-Westphalia (Germany) are often isolated remains (Diedrich 2008; Siegfried 1983).

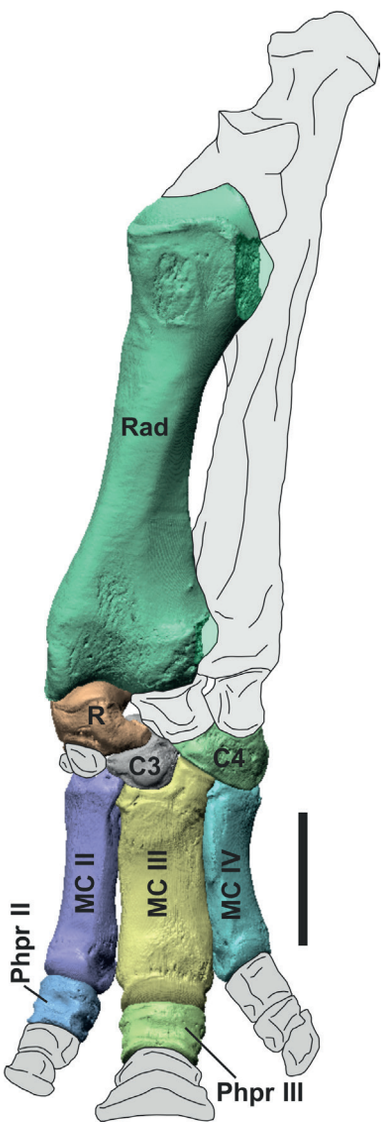

Figure 1: Polygonal models of the found woolly rhinoceros (*Coelodonta antiquitatis* WMNM P75078) bones with drawings of missing bones and missing parts of the radius. C3 - carpale 3, C4 - carpale 4, MC II - metacarpale II, MC III - metacarpale III, MC IV - metacarpale IV, Phpr II - phalanx proximalis of second digit, Phpr III - phalanx proximalis of third digit, R - radiale, Rad - radius. Scale bar 10 cm.

Adapted to cold and dry glacial climates, the woolly rhino *Coelodonta antiquitatis* had a thick coat of wool and a thick skin, a rather short tail (about 50 cm), and small ears (Boeskorov 2012). Further adaptations to cold temperatures are an elongated trunk with a considerable body weight in combination with short legs resulting in a relatively small surface (Boeskorov 2012). The nasal horn of the woolly rhino is laterally flattened and shows an abraded anterior side from removing snow cover for foraging (Boeskorov 2012; Fortelius 1983). The usage of the nasal horn and analyzed stomach content speak for a herbivorous diet made of herbs like cereals, forbs, and wormwoods (Boeskorov 2012). The reconstructed head posture and the tooth morphology of the woolly rhinoceros also speak for feeding on low vegetation (Boeskorov 2012; Borsuk-Białynicka 1973; Schellhorn 2019; Zeuner 1934, 1945). The downgrade head posture and a short and wide upper lip of the woolly rhino is also characteristic for the grazing extant white rhinoceros (Boeskorov 2012; Schellhorn 2018b).

Mammalian postcranial material shows dimensions distinct for taxa (e.g., Antoine et al. 2010; Schellhorn & Pfretzschner 2014), or for characteristic ecological adaptations (e.g., Schellhorn 2009; Schellhorn & Pfretzschner 2015; Schellhorn & Sanmugaraja 2015). As mentioned above, woolly rhinoceros remains are abundant in Westphalia, but found teeth and bones are often isolated and fragmentary. Isolated bones, such as lateral phalanges, can hardly be attributed to forelimb or hind limb because of similar shape and dimensions. The here described material belongs to one individual and offers the possibility to associate the preserved phalanges to the forelimb digits and provide measurements for these bones. Furthermore, as the ecological adaptations of the woolly rhinoceros are well studied, the bone compactness values are calculated and compared to other rhinoceros taxa whose adaptations to a terrestrial or a semiaquatic mode of life are still under debate.

Material and methods

The material with the collection number WMNM P75078 belongs to a woolly rhinoceros (*Coelodonta antiquitatis*) and consists of following bones from a left forelimb: radius, radiale, carpale 3, carpale 4, metacarpale II, metacarpale III, metacarpale IV, phalanx proximalis of metacarpale II, and phalanx proximalis of metacarpale III (Fig. 1). The material was found between August 23, 2000, (metacarpale III) and August 29, 2000, (radius; all other bones were found on August 27, 2000) by MS in the gravel pit "Kleickmann" near Wadersloh (Westphalia, Germany; Fig. 2; see also Schlösser (2012): figs 1 and 2, and Schlösser (2013a): fig 82). Back then in the year 2000, the gravel pit was actively producing

gravel and sand for construction purposes by using a floating dredge. The bones lay in close proximity to each other on a pile. According to their dimensions the bones belong to one individual. Most probably, the bones were articulated in the ground sediments of the gravel pit pond, but were disarticulated during the dredging for gravel and sand. The sediments of the "Kleickmann" gravel pit are the early to early middle Weichselian "Knochenkiese" (OIS 5d to early OIS 3), which contain not only bones of ice age mammals, but also Middle Paleolithic artifacts (Richter 2016; Schlösser 2012). The "Knochenkiese" of the "Kleickmann" gravel pit are deposits of the ancient Lippe-Ems river system (Schlösser 2013b; Ur-Lippe-Ems-Flusssystem).

RS scanned the *Coelodonta antiquitatis* (WMNM P75078) bones by micro-computed tomography (GE phoenix|x-ray v|tome|x 240s; see also Hoffmann et al. (2014) for methodology) in the Institut für Geowissenschaften, Abteilung Paläontologie (IGPB), Universität Bonn, Bonn, Germany, and reconstructed the polygonal models using the software Avizo 7.1. The carpals, metacarpals, and phalanges were scanned in one scan with a resolution of 246.37 µm. The radius was scanned in two separate scans and the produced image stacks were merged afterwards. Scan settings for all three single scans were 120 kV and 100 µA with a shutter speed of 667 ms per capture. The µCT produced isotropic voxels, and the single image size is 1024 × 1024 pixels (see Tab. 1 for scan parameters of all scanned specimens).

An abbreviated terminology is used for carpal and metacarpal bones: os carpi radiale (radiale), os carpale tertium (carpale 3), os carpale quartum (carpale 4), os metacarpale secundum (metacarpale II), os metacarpale tertium (metacarpale III), and os metacarpale quartum (metacarpale IV). For anatomical terms see NAV (2017).

Measured data (Tabs 2-10) are following sections described and/or depicted in Heissig (1972b) and Borsuk-Białynicka (1973). Comparative data are given for an extant Indian rhino (*Rhinoceros unicornis* Linnaeus, 1758) specimen (ZFMK 1988.16) and three Miocene (MN5, 16 Ma) rhinoceros species from the Bavarian locality Sandelzhausen 60 km north of Munich (Germany). The extant *Rhinoceros unicornis* specimen is housed at the Zoologisches Forschungsmuseum Alexander Koenig (ZFMK) in Bonn, Germany. The Sandelzhausen rhino specimens are belonging to three taxa: *Prosantorhinus germanicus* (Wang, 1928), *Plesiaceratherium fahlbuschi* (Heissig, 1972), and *Lartetotherium sansaniense* (Lartet, 1851). The isolated material is belonging to different individuals and is housed at the Bayerische Staatssammlung für Paläontologie und Geologie (BSPG) in Munich, Germany. The collection numbers of the Sandelzhausen fossils have the prefix BSPG 1959 II.

Figure 2: Map of Germany with labeled locality Wadersloh (Westphalia).

Bone compactness is used as a tool to differentiate between (semi-)aquatic and terrestrial taxa (e.g., Germain & Laurin 2005; Houssaye & Bardet 2012; Houssaye & Botton-Divet 2018; Laurin et al. 2011; Nakajima & Endo 2013). This parameter is the ratio of the area of solid bone tissue to the total sectional area (de Buffrénil et al. 2010). The different areas of the cross sections were measured using the software FIJI (FIJI is just ImageJ 1.51u; Abramoff et al. 2004; Schneider et al. 2012). The cross sections (Fig. 3) were taken from the mid-diaphysis where the thickest cortex occurs in long bones (Sander & Andrássy 2006). Bone compactness (Tab. 1) was calculated for the scanned radii and metacarpals of the present *Coelodonta antiquitatis* material, as well as the above mentioned Sandelzhausen rhinoceros species, and an extant pygmy hippo (*Choeropsis liberiensis* (Morton, 1849), ZFMK 65.570) for comparison. The pygmy hippo has a semiaquatic lifestyle, but is less water dependent than the common hippopotamus (Flacke & Decher 2019; Wall 1983).

Institutional abbreviations

BSPG	Bayerische Staatssammlung für Paläontologie und Geologie, München, Germany
IGPB	Institut für Geowissenschaften, Abteilung Paläontologie, Rheinische Friedrich-Wilhelms-Universität Bonn, Bonn, Germany
WMNM	LWL-Museum für Naturkunde, Westfälisches Landesmuseum mit Planetarium, Münster, Germany
ZFMK	Zoologisches Forschungsmuseum Alexander Koenig, Bonn, Germany

Tab. 1: Scan parameters for all specimens and bone compactness values for radii and metacarpals. The µCT produced isotropic voxels, and the single image size is 1024×1024 pixels for all scans.

	resolution	voltage	current	shutter speed	bone compactness
Coelodonta antiquitatis					
WMNM P75078					
radius sin.	246.370 µm	120 kV	100 µA	667 ms	77.0 %
MC II sin.	246.370 µm	120 kV	100 µA	667 ms	46.5 %
MC III sin.	246.370 µm	120 kV	100 µA	667 ms	57.6 %
MC IV sin.	246.370 µm	120 kV	100 µA	667 ms	55.3 %
radiale sin, C3 sin., C4 sin., prox. phalanx II sin., prox. phalanx III sin.	246.370 µm	120 kV	100 µA	667 ms	---
Choeropsis liberiensis					
ZFMK 65.570					
radius dex.	246.370 µm	180 kV	150 µA	400 ms	79.8 %
MC II dex.	246.370 µm	180 kV	150 µA	400 ms	57.2 %
MC III dex.	246.370 µm	180 kV	150 µA	400 ms	57.7 %
MC IV dex.	246.370 µm	180 kV	150 µA	400 ms	55.9 %
Lartetotherium sansaniense					
BSPG 1959 II 17085, MC II sin.	246.370 µm	180 kV	150 µA	500 ms	77.7 %
BSPG 1959 II 17087, MC III sin.	246.370 µm	180 kV	150 µA	500 ms	63.7 %
BSPG 1959 II 17086, MC IV sin.	246.370 µm	180 kV	150 µA	500 ms	69.2 %
Plesiaceratherium fahlbuschi					
BSPG 1959 II 17071, MC IV dex.	246.370 µm	180 kV	150 µA	333 ms	71.3 %
Prosantorhinus germanicus					
BSPG 1959 II 12272, MC II sin.	146.997 µm	180 kV	150 µA	500 ms	58.5 %
BSPG 1959 II 17005, MC III dex.	246.370 µm	180 kV	150 µA	333 ms	55.5 %
BSPG 1959 II 17007, MC IV dex.	246.370 µm	180 kV	150 µA	333 ms	68.3 %

Systematic paleontology

Order: Perissodactyla Owen, 1848
Suborder: Mesaxonia Marsh, 1884
Infraorder: Tapiromorpha Haeckel, 1873
Parvorder: Ceratomorpha Wood, 1937
Superfamily: Rhinocerotoidea Gray, 1821
Family: Rhinocerotidae Gray, 1821
Subfamily: Rhinocerotinae Gray, 1821
Tribe: Rhinocerotini Gray, 1821
Subtribe: Rhinocerotina Gray, 1821
Genus: *Coelodonta* Bronn, 1831
Species: *Coelodonta antiquitatis* (Blumenbach, 1799)

Description

Radius sin. (Tab. 2, Pl. I A-F): The radius is a relatively straight bone and nearly completely preserved. The lateral part of the proximal end (lateraler Bandhöcker, tuberositas proximalis lateralis after Sisson (1914), the insertion place of the ligamentum collaterale laterale) is broken off, as well as the caudal and lateral bony surfaces of the distal end. This long bone shows a bent cranial surface from proximolateral to distomedial. The cranial surface proximally shows a rounded rugose area (tuberositas radii, around 5 cm in diameter), the insertion place for the musculus biceps brachii. Distally to the tuberositas

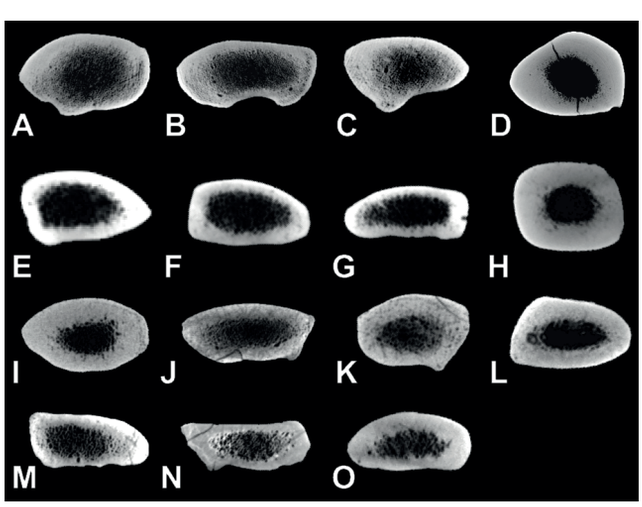

Figure 3: Mid-diaphyseal cross sections of examined bones of *Coelodonta antiquitatis* (**A-D**), *Choeropsis liberiensis* (**E-H**), *Lartetotherium sansaniense* (**I-K**), *Plesiaceratherium fahlbuschi* (**L**), and *Prosantorhinus germanicus* (**M-O**). A MC II sin., *Coelodonta antiquitatis* (WMNM P75078), B MC III sin., *Coelodonta antiquitatis* (WMNM P75078), C MC IV sin., *Coelodonta antiquitatis* (WMNM P75078), D radius sin., *Coelodonta antiquitatis* (WMNM P75078), E MC II dex., *Choeropsis liberiensis* (ZFMK 65.570), F MC III dex., *Choeropsis liberiensis* (ZFMK 65.570), G MC IV dex., *Choeropsis liberiensis* (ZFMK 65.570), H radius dex., *Choeropsis liberiensis* (ZFMK 65.570), I MC II sin., *Lartetotherium sansaniense* (BSPG 1959 II 17085), J MC III sin., *Lartetotherium sansaniense* (BSPG 1959 II 17087), K MC IV sin., *Lartetotherium sansaniense* (BSPG 1959 II 17086), L MC IV dex., *Plesiaceratherium fahlbuschi* (BSPG 1959 II 17071), M MC II sin., *Prosantorhinus germanicus* (BSPG 1959 II 12272), N MC III dex., *Prosantorhinus germanicus* (BSPG 1959 II 17005), O MC IV dex., *Prosantorhinus germanicus* (BSPG 1959 II 17007). Sections are not to scale.

radii, a medially oriented oval tuberosity (around 6 cm in proximal-distal axis) is visible, the insertion area of the musculus brachialis (see fig. 8 in Borsuk-Białynicka (1973)). The facies caudalis of the corpus radii shows two rugosities to contact the not-preserved ulna by interosseous ligaments or membranes. The proximal rugosity is slightly concave, while the distal one is flat and oval in shape. Proximal to the distal contact area a foramen nutricium is situated. Lateral to this foramen nutricium and the distal contact area with the ulna, a distinct groove for a vessel and/or nerve is visible. The lateral border of this groove is formed by the margo lateralis of the radius. As mentioned above the lateral part of the caput radii is broken off. Therefore, only the medial part of the fovea capitis radii, the articulation with the humerus, is preserved. This medial part is more or less quadrate shaped and concave. This depression ascends to a smooth ridge separating the medial part of the fovea capitis radii from the not-preserved lateral part. The distal end of the radius shows the articulation facets with the preserved radiale and the not-preserved intermedium (os carpi intermedium). The medial articulation facet for the radiale is cranially concave, changing over to a convex surface caudally, and is medially bordered by the processus styloideus medialis. The laterally situated articulation facet with the intermedium is a shallow concavity while the caudal part is broken off.

Radiale sin. (Tab. 3, Pl. I G-J): The radiale is one of the larger carpal bones. Nearly the whole proximal surface consists of the articulation facet with the radius. This facet is mediopalmar a wider concave channel ascending to a convex structure close to the dorsal plane of the radiale. This proximal facet bends towards the lateral plane into two facets with the intermedium. The dorsal facet is shallow and long, while the palmar facet is triangular in shape. Both facets are connected by a small ridge. A third facet on the lateral plane is located dorsodistally. This facet also contacts the intermedium and has an elongated shape, and is pointing towards a lateropalmar direction. On the distal plane there are three articulation facets with the carpale 1, carpale 2, and carpale 3 (from medial to lateral). All three facets are connected by dorsal to palmar ridges. The carpale 1 facet is the smallest of these three facets and is of semicircular shape. The carpale 2 facet is the largest and is smoothly bent onto the dorsal plane. The carpale 3 facet, the lateral facet, is triangular to trapezoid in shape and is connected to the distal intermedium facet on the lateral plane of the radiale.

Carpale 3 sin. (Tab. 4, Pl. II A-E): The carpale 3 is a long, slender, and shallow bone. In general, the dorsal part of the bone is the part with the articulation facets with different bones, and the palmar part is a hook without any facet. This palmar hook is slightly bent distally and medially. An apparent structure is the nearly hemispheric proximal articulation with the intermedium. This proximal hemispheric articulation facet is dorsally in contact with the articulation facet with the carpale 4 (laterally situa-

Tab. 2: Measurements of the radius (sin.) of *Coelodonta antiquitatis* (WMNM P75078) and comparative data of *Coelodonta antiquitatis* (published data from Borsuk-Białynicka (1973)) and other rhinoceros taxa.

	Coelodonta antiquitatis	*Coelodonta antiquitatis*	*Rhinoceros unicornis*	*Prosantorhinus germanicus*	*Plesiaceratherium fahlbuschi*	*Lartetotherium sansaniense*
	WMNM P75078	(Borsuk-Białynicka 1973, tab. 41, p. 68)	ZFMK 88.16	BSPG 1959 II 18142	BSPG 1959 II 18132	BSPG 1959 II 18103
			dex.	sin.	dex.	sin.
greatest length	403 mm	343-385 mm	418 mm	214 mm	331 mm	335 mm
lateral-medial width of proximal end	---	102-117 mm	127 mm	62 mm	69 mm	86 mm
cranial-caudal depth of proximal end	70 mm	---	89 mm	40 mm	47 mm	56 mm
lateral-medial width of distal end	119 mm	110 mm	132 mm	59 mm	66 mm	79 mm
cranial-caudal depth of distal end	81 mm	---	85 mm	35 mm	51 mm	51 mm

Tab. 3: Measurements of the radiale (sin.) of *Coelodonta antiquitatis* (WMNM P75078) and comparative data of *Coelodonta antiquitatis* (published data from Borsuk-Białynicka (1973)) and other rhinoceros taxa.

	Coelodonta antiquitatis	*Coelodonta antiquitatis*	*Rhinoceros unicornis*	*Prosantorhinus germanicus*	*Plesiaceratherium fahlbuschi*	*Lartetotherium sansaniense*
	WMNM P75078	(Borsuk-Białynicka 1973, tab. 43, p. 73)	ZFMK 88.16	BSPG 1959 II 12030	BSPG 1959 II 17048	BSPG 1959 II 17075
			dex.	sin.	dex.	dex.
width	94 mm	86 mm	85 mm	44 mm	37 mm	40 mm
height	63 mm	60 mm	80 mm	33 mm	54 mm	52 mm
depth (thickness)	67 mm	69 mm	70 mm	45 mm	60 mm	67 mm

ted) and the facet with the radiale (medially situated). The carpale 4 facet is rectangular in shape while the radiale facet is more triangular in shape. On the medial plane there are two articulation facets. The proximal facet, pointing in a dorsomedial direction, is the articulation facet with the carpale 2. Distally to this facet there is the long and slender facet with the metacarpale II. The distal plane only bears one concave facet with the metacarpale III. The facets on the dorsal part of the carpale 3 are connected by distinct ridges. The dorsal plane of the bone shows a proximal edge and a proximolateral edge, while the medial and distal border of this plane is semicircular in shape.

Carpale 4 sin. (Tab. 5, Pl. II F-J): The carpale 4 shows a massive dorsal part of the bone, which is surrounded by articulation facets and a palmar part of the bone without any facet. The palmar part is a hook which is bent laterally and slightly distally. The dorsal plane of the carpale 4 is nearly rectangular in shape. The proximal articulation facet on the carpale 4 is convexly bent from dorsal to palmar and nearly rectangular in shape. This articulation facet bears the ulnare. This facet is medially connected by a ridge to the intermedium facet which points proximomedially. This facet connects by a ridge to a large distal facet. This distal facet extends on the lateral plane and contacts to three bones without a clearly visible separation between these three contact facets. The medial part of this large facet is sitting on the carpale 3. The middle (and largest) part of this large facet contacts the metacarpale IV. The lateral part of the large facet (also facing laterally) contacts the leftover of the metacarpale V. This metacarpale V is not preserved, but is most probably a small ball-like shaped bone, like it is in *Rhinoceros unicornis* for example.

Metacarpale II sin. (Tab. 6, Pl. III A-F): The metacarpale II is a long and slender bone with a set of articulation facets on its proximal end and one facet on its distal end. The largest proximal articulation facet, a saddle-like facet, contacts the carpale 2. Laterally adjacent, connected by a ridge, is the facet with the carpale 3. This facet is elongated and slender, and is pointing in a proximolateral direction. The lateral facet on the proximal end of the metacarpale II is triangular or semicircular in shape and contacts the metacarpale III. This facet and also a part of the bone are caudally slightly bent around the metacarpale III. The shaft of the metacarpale II is triangular in cross section. In the middle part of the caudal plane there is a foramen nutricium laterally, a groove for a blood vessel medially, and a rugosity between both structures. The distal part of the bone is formed by an articulation facet (a trochlea) with the proximal phalanx. This facet starts on the dorsal plane and ends on the palmar plane with a sagittal ridge on the palmar part. Medial and lateral to this sagittal ridge a sesamoid bone is attached to the trochlea. Shallow depressions are visible where the two sesamoid bones articulated. The medial and lateral planes of the trochlea are shallow depressions.

Metacarpale III sin. (Tab. 7, Pl. III G-L): The metacarpale III is the largest metacarpal bone and has a nearly oval shape in cross section. The proximal end of the bone articulates with four other bones. The largest and proximal oriented articulation facet with the carpale 3 has a saddle-like structure. Lateral to this facet an elevated triangular shaped facet contacts the carpale 4 and points to a proximomedial direction. The carpale 3 and the carpale 4 facets are connected via a ridge. On the lateral plane of the proximal end two facets to the metacarpale IV are visible. Both facets are nearly perpendicular to each other. The dorsal facet is semicircular in shape and via a ridge connected to the carpale 4 facet. The palmar facet is round to slightly oval in shape and separated from the other facets. The facet on the medial plane of the proximal end is rectangular in shape and contacts the metacarpale II. This facet points in a proximomedial direction and is connected to the carpale 3 facet via a ridge. The dorsal plane of the proximal end shows a larger rugosity. The palmar plane of the corpus metacarpale shows an elongated proximal to distal oriented depression and a foramen nutricium in the proximal part of the medial border of this depression. The distal part of the metacarpale III is formed by a trochlea articulating with the proximal phalanx of the third digit. The palmar part of this trochlea is divided by a ridge in two parts articulating with a medial and lateral sesamoid bone. Shallow depressions of the oval shaped articulation facets are visible.

Metacarpale IV sin. (Tab. 8, Pl. IV A-F): The metacarpale IV is the smallest of the functional metacarpal bones. It also shows a slight curvature from proximal to distal and is triangular in cross section. The proximal end of the bone articulates with two other bones. The large triangular to trapezoid proximal articulation facet with the carpale 4 is shallow concave. This facet connects by a ridge medially to the two articulation facets with the metacarpale III. The dorsal facet is elongated semicircular in shape while the palmar facet is round. Both facets are also connected by a ridge and span an angle of around 270° to each other. The lateral part of the proximal end is badly preserved, but probably there was a small facet with the reduced metacarpale V, like this is the case in the extant *Rhinoceros unicornis*. The medial plane of the corpus metacarpale bears a large bulbous rugosity in the proximal half of the shaft. The palmar plane of the corpus shows a medial foramen nutricium close to distal end of this rugosity. The distal part of the shaft's dorsal

Tab. 4: Measurements of the carpale 3 (sin.) of *Coelodonta antiquitatis* (WMNM P75078) and comparative data of *Coelodonta antiquitatis (*published data from Borsuk-Białynicka (1973)) and other rhinoceros taxa.

	Coelodonta antiquitatis	*Coelodonta antiquitatis*	*Rhinoceros unicornis*	*Prosantorhinus germanicus*	*Plesiaceratherium fahlbuschi*	*Lartetotherium sansaniense*
	WMNM P75078	(Borsuk-Białynicka 1973, tab. 43, p. 73)	ZFMK 88.16	BSPG 1959 II 12205	BSPG 1959 II 17034	BSPG 1959 II 17074
			dex.	dex.	dex.	sin.
dorsal width (greatest width)	56 mm	49 mm	65 mm	35 mm	39 mm	46 mm
dorsal height	39 mm	25 mm	42 mm	19 mm	30 mm	32 mm
greatest height	68 mm	---	75 mm	35 mm	53 mm	58 mm
depth (thickness)	108 mm	89 mm	107 mm	55 mm	74 mm	79 mm

Tab. 5: Measurements of the carpale 4 (sin.) of *Coelodonta antiquitatis* (WMNM P75078) and comparative data of *Coelodonta antiquitatis* (published data from Borsuk-Białynicka (1973)) and other rhinoceros taxa.

	Coelodonta antiquitatis	*Coelodonta antiquitatis*	*Rhinoceros unicornis*	*Prosantorhinus germanicus*	*Plesiaceratherium fahlbuschi*	*Lartetotherium sansaniense*
	WMNM P75078	(Borsuk-Białynicka 1973, tab. 43, p. 73)	ZFMK 88.16	BSPG 1959 II 12230	BSPG 1959 II 17041	BSPG 1959 II 17111
			dex.	dex.	sin.	dex.
dorsal width	81 mm	66 mm	84 mm	39 mm	50 mm	64 mm
dorsal height (greatest height)	52 mm	48 mm	60 mm	27 mm	37 mm	46 mm
depth (thickness)	90 mm	75 mm	95 mm	44 mm	56 mm	62 mm

Tab. 6: Measurements of the metacarpale II (sin.) of *Coelodonta antiquitatis* (WMNM P75078) and comparative data of *Coelodonta antiquitatis* (published data from Borsuk-Białynicka (1973)) and other rhinoceros taxa.

	Coelodonta antiquitatis	*Coelodonta antiquitatis*	*Rhinoceros unicornis*	*Prosantorhinus germanicus*	*Plesiaceratherium fahlbuschi*	*Lartetotherium sansaniense*
	WMNM P75078	(Borsuk-Białynicka 1973, tab. 44, p. 75)	ZFMK 88.16	BSPG 1959 II 12272	BSPG 1959 II 17091	BSPG 1959 II 17085
			dex.	sin.	sin.	sin.
greatest length	170 mm	---	189 mm	77 mm	161 mm	154 mm
lateral-medial width of proximal end	61 mm	51 mm	58 mm	27 mm	37 mm	39 mm
dorsal-palmar depth of proximal end	46 mm	---	49 mm	25 mm	---	34 mm
lateral-medial width of distal end	51 mm	48 mm	51 mm	26 mm	31 mm	35 mm
dorsal-palmar depth of distal end	48 mm	---	48 mm	26 mm	35 mm	35 mm

Tab. 7: Measurements of the metacarpale III (sin.) of *Coelodonta antiquitatis* (WMNM P75078) and comparative data of *Coelodonta antiquitatis* (published data from Borsuk-Białynicka (1973)) and other rhinoceros taxa.

	Coelodonta antiquitatis	*Coelodonta antiquitatis*	*Rhinoceros unicornis*	*Prosantorhinus germanicus*	*Plesiaceratherium fahlbuschi*	*Lartetotherium sansaniense*
	WMNM P75078	(Borsuk-Białynicka 1973, tab. 44, p. 75)	ZFMK 88.16	BSPG 1959 II 17005	BSPG 1959 II 17092	BSPG 1959 II 17087
			dex.	dex.	sin.	sin.
greatest length	197 mm	161 mm	225 mm	95 mm	171 mm	174 mm
lateral-medial width of proximal end	74 mm	60 mm	79 mm	39 mm	46 mm	51 mm
dorsal-palmar depth of proximal end	53 mm	---	59 mm	30 mm	40 mm	42 mm
lateral-medial width of distal end	73 mm	57 mm	70 mm	35 mm	38 mm	43 mm
dorsal-palmar depth of distal end	54 mm	---	54 mm	28 mm	32 mm	43 mm

Tab. 8: Measurements of the metacarpale IV (sin.) of *Coelodonta antiquitatis* (WMNM P75078) and comparative data of *Coelodonta antiquitatis* (published data from Borsuk-Białynicka (1973)) and other rhinoceros taxa.

	Coelodonta antiquitatis	*Coelodonta antiquitatis*	*Rhinoceros unicornis*	*Prosantorhinus germanicus*	*Plesiaceratherium fahlbuschi*	*Lartetotherium sansaniense*
	WMNM P75078	(Borsuk-Białynicka 1973, tab. 44, p. 75)	ZFMK 88.16	BSPG 1959 II 17007	BSPG 1959 II 17071	BSPG 1959 II 17086
			dex.	dex.	dex.	dex.
greatest length	153 mm	---	179 mm	78 mm	132 mm	136 mm
lateral-medial width of proximal end	56 mm	44 mm	60 mm	29 mm	23 mm	37 mm
dorsal-palmar depth of proximal end	48 mm	---	55 mm	30 mm	31 mm	33 mm
lateral-medial width of distal end	48 mm	43 mm	54 mm	27 mm	27 mm	31 mm
dorsal-palmar depth of distal end	45 mm	---	46 mm	26 mm	31 mm	30 mm

plane shows a depression. The distal end of the metacarpale IV is formed by a trochlea from the dorsal plane to the palmar plane. The part on the dorsal plane articulates with the proximal phalanx of the fourth digit, while the part on the palmar plane is divided by a ridge in a larger lateral facet and a smaller medial facet. Both facets show shallow depressions for articulation with sesamoid bones.

Phalanx proximalis of anterior digitus II sin. (Tab. 9, Pl. IV G-L): The proximal phalanx of the second digit shows a proximal concave oval shaped articulation facet (fovea articularis) with the metacarpale II. The distal plane is also completely consisting of one articulation facet. This rather flat facet articulates with the phalanx media of the second digit and is rectangular in shape with round edges and a palmar insertion. The basis phalangis shows a greater dorsal to palmar depth than the caput phalangis. The lateral plane of the bone is nearly flat while the medial plane is slightly convex giving this phalanx an asymmetric shape.

Phalanx proximalis of anterior digitus III sin. (Tab. 10, Pl. IV M-R): The proximal phalanx of the third digit is symmetrical to the sagittal plane. The proximal fovea articularis is the facet with the metacarpale III. Close to this facet on the palmar plane there are proximally two shallow depressions which most probably originate from the distal sesamoid bones of the metacarpale III. The proximal fovea articularis is oval in shape with a shallow insertion on the palmar edge. The distal articulation facet is slightly convex and articulates with the phalanx media of the third digit. This articulation facet is nearly rectangular in shape. The proximal basis phalangis shows a greater dorsal to palmar depth than the distal caput phalangis.

Bone compactness

The radius (Fig. 3D) of the Pleistocene woolly rhino *Coelodonta antiquitatis* shows a higher percentage (Tab 1.: 77.0 %) of compact bone than the metacarpals (Figs. 3A-C; MC II: 46.5 %, MC III: 57.6 %; MC IV: 55.3%). These values are comparable to the data of the extant pygmy hippo *Choeropsis liberiensis* (Tab. 1; Figs. 3E-H). The radius has a much greater value of 79.8 % where the metacarpals show values between 55.9 % and 57.7 %. While the metacarpal bone compactness data of the woolly rhino and the pygmy hippo are all below 60 % (and the radius values are close to 80 %), the values of the Miocene Sandelzhausen rhino metacarpals are ranging between 55.5 % and 77.7 % (Tab. 1). Among the Sandelzhausen rhinos the largest species (*Lartetotherium sansaniense*) trends to show greater bone compactness values (63.7–77.7 %) and the smallest species (*Prosan-*

Tab. 9: Measurements of the phalanx proximalis of the second digit (sin.) of *Coelodonta antiquitatis* (WMNM P75078), and comparative data of *Rhinoceros unicornis*.

	Coelodonta antiquitatis	*Rhinoceros unicornis*
	WMNM P75078	ZFMK 88.16
		dex.
greatest height	51 mm	58 mm
lateral-medial width of proximal end	48 mm	51 mm
dorsal-palmar depth of proximal end	41 mm	46 mm
lateral-medial width of distal end	46 mm	46 mm
dorsal-palmar depth of distal end	33 mm	35 mm

Tab. 10: Measurements of the phalanx proximalis of the third digit (sin.) of *Coelodonta antiquitatis* (WMNM P75078) and comparative data of *Rhinoceros unicornis*.

	Coelodonta antiquitatis	*Rhinoceros unicornis*
	WMNM P75078	ZFMK 88.16
		dex.
greatest height	48 mm	54 mm
lateral-medial width of proximal end	64 mm	75 mm
dorsal-palmar depth of proximal end	43 mm	51 mm
lateral-medial width of distal end	57 mm	68 mm
dorsal-palmar depth of distal end	32 mm	34 mm

torhinus germanicus) trends to show smaller values (55.5–68.3 %). For *Plesiaceratherium fahlbuschi* only one metacarpal IV could be analyzed and the value of 71.3 % is close to the MC IV values of the other two Sandelzhausen taxa (see Tab. 1).

Discussion

Taxonomic identification of the Wadersloh material

The assignment of the found remains to the species *Coelodonta antiquitatis* is due to found woolly rhinoceros dental remains from the same gravel pit and also found remains of other glacial faunal elements like woolly mammoth, reindeer, polar fox, and musk ox (Schlösser 2012). The age of the Wadersloh locality is dated to the Weichselian glacial period (Middle Paleolithic; Baales 2012; Richter 2016; Schlösser 2012). If the attribution to the glacial period would not be correct the found remains could also belong to an interglacial species of *Stephanorhinus*. Lengths of here described radius and metacarpals fall in the range of *Stephanorhinus* taxa, but the measurements of breadths and depths of the here discussed bones of *Coelodonta* show greater values compared to the species of *Stephanorhinus* (compare tabs 12, 20, 21, and 22 in Fortelius et al. (1993)). Comparative woolly rhino figures and tables show similar anatomical features and measurements to the here presented data (see figs 90–94, 95–100 and tabs 130, 132, 137–141 in Guérin (1980)). The comparative woolly rhino data (Tabs 2-8) taken from Borsuk-Białynicka (1973) show smaller values for lengths, widths, and depths of long bones and carpals compared to the presented material. Phalangeal measurements are not provided by Borsuk-Białynicka (1973). The smaller appearance of the Borsuk-Białynicka (1973) material might be due to the fact that this woolly rhino material originates from more eastern Eurasian regions like Poland and the former USSR. Middle Pleistocene woolly rhino material attributed to *Coelodonta tologoijensis* is also more slender than late Pleistocene *Coelodonta antiquitatis* material (Kahlke & Lacombat 2008). The late Pliocene *Coelodonta nihowanensis* displays much more slender metacarpals than *C. antiquitatis* and also *C. tologoijensis* (Deng 2006, 2008).

Bone compactness

As the material in this study belongs to one woolly rhino individual, the investigation of bone compactness of radius and metacarpals seems appropriate. In extant taxa there is a difference in bone compactness values between terrestrial (smaller values) and aquatic forms (greater values) visible which is also used to state about the ecology of fossil taxa (e.g., de Buffrénil et al. 2010; Houssaye & Bardet 2012; Laurin et al. 2011). Subject of such microanatomical studies are often ribs and long bones of the limbs (e.g., Canoville et al. 2016; Houssaye & Botton-Divet 2018; Houssaye et al. 2016; Kriloff et al. 2008). In this study the bone compactness of radius (77.0 %) and metacarpals (46.5–57.6 %) of the woolly rhino and the extant pygmy hippo (radius: 79.8 %; metacarpals: 55.9–57.7 %) were analyzed. The values of the radii are greater than the values of the metacarpals, but interestingly the values are very similar in both taxa, and as stated above the woolly rhino is an undoubtedly terrestrial taxon, while the pygmy hippo shows a semiaquatic lifestyle (Flacke & Decher 2019). Wall (1983) determined the percentage of compact bone in limb elements of the terrestrial extant white rhino and the two extant hippo species. His methodology was slightly different to this study, therefore the values are not comparable, but in his sample the values of the humeri of the terrestrial white rhino versus the two semiaquatic hippo taxa are in the same range (Wall 1983). For radius, femur, and tibia smaller values are reported for the white rhino than for the two extant hippo species (Wall 1983). There is no difference between the bone compactness of the terrestrial woolly rhino and the semiaquatic pygmy hippo visible in our sample. Furthermore, the Miocene rhino specimens show even greater values for metacarpal bone compactness as the pygmy hippo does. Therefore, bone compactness might not be very useful to differentiate between terrestrial and semiaquatic rhinoceros taxa. For the extant Javan rhino (*Rhinoceros sondaicus*) it was reported before that this taxon shows an unusually thick cortex and a great bone compactness value for a terrestrial mammal (Canoville et al. 2016; de Buffrénil et al. 2010). It is undebated that rhinos are wallowing and dependent from water (e.g., Groves 1972; Groves & Kurt 1972; Groves & Leslie 2011; Laurie et al. 1983; Owen-Smith 988), and the Javan rhinoceros is sometimes even considered as semiaquatic (Benoit et al. 2020). So maybe the cortex is not unusually thick in terrestrial rhinos, but rhinos are somewhat intermediate in their mode of life between terrestrial and semiaquatic. As Yalden (1971) notes, the rhinoceros carpus differs in some respect from that of the horse like the hippo carpus differs from that of ruminants. In shorter footed animals like rhinos and hippos the wrist joint flexion is primarily produced at the proximal joint (Yalden 1971). This seems to be also the case in the here presented *Coelodonta* remains. Beside the degree of adaptation to moist environments, the great bone compactness of rhinos and other terrestrial taxa is also linked to graviportality (e.g., Houssaye et al. 2016; Sander et al. 2011). In their sample Houssaye et al. (2016) show compactness values of extant and fossil rhinos in the same range or even greater than extant hippos for humeri, femora,

and ribs. For some authors the woolly rhino is also a graviportal taxon or shows at least several graviportal adaptations (e.g., Borsuk-Białynicka 1973; Kahlke & Lacombat 2008). Other authors see rhinos and hippos as mediportal taxa (e.g., Gregory 1912; Schellhorn 2018a), but this will be discussed elsewhere.

Ecological implications for the Sandelzhausen rhinoceroses
Rhinoceros remains are the most abundant vertebrate remains in the Miocene Sandelzhausen locality. *Prosantorhinus germanicus* is the smallest and most abundant species (Heissig 1972a). *Plesiaceratherium fahlbuschi* is medium sized and nearly as abundant as *P. germanicus*, while the largest species, *Lartetotherium sansaniense*, is scarce (Heissig 1972a). Belonging to the tribe Teleoceratini, a hippo-like mode of life was assumed for *Prosantorhinus germanicus* (Heissig 1999). Comparing the bone compactness data for the metacarpals in this study (Tab. 1), there is no significant difference between the Sandelzhausen rhino taxa and the extant pygmy hippo visible. While the *P. germanicus* data are close to the pygmy hippo data, the bone compactness values of *L. sansaniense* and *P. fahlbuschi* are greater than the pygmy hippo data. This would indicate a more semi-aquatic lifestyle than in the extant pygmy hippo what most probably is not the case. The misleading results might be an effect of taphonomy and preservation of the Miocene rhino material. Then the bones would show a larger area of compact bone than actually present due to mineral aggregation added to the compact bone showing the same density as true bone material in the x-ray images (Fig. 3). This seems very unlikely, because broken bones do not show any mineral crystals just bone material. But putting the focus just on the three Miocene taxa, which are all affected by the same taphonomic processes, the mode of life of *P. germanicus* is assumed to be closer to a hippo lifestyle than the other two taxa (Heissig 1972a). With smaller bone compactness values this assumption is not supported, in turn this would indicate a more terrestrial mode of life than for the other two taxa. According to Heissig (1972a) all three Sandelzhausen rhinoceros taxa are faunal elements of moist environments, while *P. germanicus* liked it more moist than *P. fahlbuschi* and *L. sansaniense*. As mentioned above, *P. germanicus* belongs to the tribe Teleoceratini like the type genus *Teleoceras*. For *Teleoceras* also a hippo-like mode of life was proposed (e.g., Prothero 1998). Like in hippos, the typical teleoceratine anatomy shows a robust skeleton with short limbs (Prothero 1998). Following Mihlbachler (2005) there is no direct support that *Teleoceras* had a behavior like hippos. Isotope studies also do not support aquatic habits for *Teleoceras* (Clementz et al. 2008). As Boeskorov (2012) noted, there are also an elongated trunk and relatively short legs present in the woolly rhino *Coelodonta antiquitatis*, and there is no doubt that the woolly rhino was a terrestrial species.

Following isotope studies, the Sandelzhausen environment was a swampy area gradually changing to a perennial lake (Salvador et al. 2018). The terrestrial habitat changed from a relatively open semi-arid/sub-humid scrubland to a sub-humid/humid denser forest (Salvador et al. 2018). Tütken & Vennemann (2009) analyzed the isotopic composition of mammal teeth from the Sandelzhausen locality including the three sympatric rhinoceros taxa. Similar mean enamel $\delta^{18}O$ values show a water-dependence of the three taxa (Tütken & Vennemann 2009), but compared to the associated fauna the rhinos show intermediate values between an equid and a cervid for example, and therefore there is no support for a hippo-like mode of life. As there are no hippos known from Sandelzhausen a direct comparison of isotopic data towards a semiaquatic mode of life is not possible. Such a comparison of isotopic data of the woolly rhino and a contemporaneous hippo from the same locality is also not possible, because the Pleistocene hippos only occurred in the interglacial periods (Kurtén 1968). New tooth enamel $\delta^{18}O$ data do also not support the interpretation that *Teleoceras* had a semiaquatic lifestyle (Wang & Secord 2020).

Conclusions
The distal bones of a left forelimb (radius, three carpals, three metacarpals, and two phalanges) of a late Pleistocene woolly rhinoceros *(Coelodonta antiquitatis*) are described in detail. The bones with the collection number WMNM P75078 are found in the gravel pit "Kleickmann" near Wadersloh (Westphalia, Germany). Measurements are given and because of their dimensions and the finding situation the bones are belonging to one individual. These remains are the most complete articulated remains of a woolly rhino for the Wadersloh area. Radius and metacarpals are furthermore scanned by micro-computed tomography to calculate the bone compactness value. Comparative data are collected from an extant pygmy hippo and the metacarpals of three rhinoceros taxa from the Miocene locality Sandelzhausen (Bavaria, Germany). The bone compactness values are compared between the terrestrial woolly rhino and the semiaquatic pygmy hippo. Both taxa show similar values while the radii are more compact than the metacarpals. The Sandelzhausen rhinos show comparable or even greater values for their metacarpals. This would indicate an even higher degree of adaptation towards an aquatic environment than in the pygmy hippo. Water dependency was proposed before for the Sandelzhausen

rhinos, but as already the terrestrial woolly rhino shows bone compactness values like the pygmy hippo, bone compactness seems not to be the best tool to differentiate between terrestrial and semiaquatic rhinos. The high degree of compact bone in rhinos was mentioned before and might be a result of the large body weight. But on the other hand, wallowing is an important behavior what shows the water dependency in extant and fossil rhinos.

Acknowledgements

We thank Achim H. Schwermann (WMNM) for loan of the Wadersloh material, Gertrud Rössner and Kurt Heissig (both BSPG) for loan of the Sandelzhausen material, and Rainer Hutterer and Jan Decher (both ZFMK) for loan of comparative material. Thanks to Georg Oleschinski (IGPB) for preparing the photographs. We thank Mikael Fortelius and Tao Deng for their helpful comments greatly improving the manuscript. RS received funding through the Deutsche Forschungsgemeinschaft (DFG, German Research Foundation) – SCHE 1882/1-1.

References

Abramoff, M.D., Magalhaes, P.J. & Ram, S.J. 2004: Image processing with ImageJ. - Biophotonics International 11 (7): 36-42.

Antoine, P.-O., Downing, K.F., Crochet, J.-Y., Duranthon, F., Flynn, L.J., Marivaux, L., Métais, G., Rajpar, A.R. & Roohi, G. 2010: A revision of *Aceratherium blanfordi* Lydekker, 1884 (Mammalia: Rhinocerotidae) from the Early Miocene of Pakistan: postcranials as a key. - Zoological Journal of the Linnean Society 160: 139-194.

Baales, M. 2012. Late Middle Palaeolithic artefacts and archaeostratigraphical dating of the bone gravels (Knochenkiese) in Central Westphalia and the Ruhrgebiet (Germany). In: Niekus, M. J. L. T., Barton, N., Street, M. & Terberger, T., eds.), A mind set on flint - studies in honour of Dick Stapert, 119-139. Groningen: Barkhuis.

Benoit, J., Legendre, L.J., Farke, A.A., Neenan, J.M., Mennecart, B., Costeur, L., Merigeaud, S. & Manger, P.R. 2020: A test of the lateral semicircular canal correlation to head posture, diet and other biological traits in „ungulate" mammals. - Scientific Reports 10 (1): 19602.

Blumenbach, J.F. 1799: Handbuch der Naturgeschichte. Göttingen: Johann Christian Dieterich.

Boeskorov, G.G. 2012: Some specific morphological and ecological features of the fossil woolly rhinoceros (*Coelodonta antiquitatis* Blumenbach 1799). - Biology Bulletin 39 (8): 692-707.

Borsuk-Białynicka, M. 1973: Studies on the Pleistocene rhinoceros *Coelodonta antiquitatis* (Blumenbach). - Palaeontologia Polonica 29: 1-94.

Bronn, H.G. 1831: Über die fossilen Zähne eines neuen Geschlechtes aus der Dickhäuter-Ordnung, *Coelodonta*, Höhlenzahn. - Jahrbuch für Mineralogie, Geognosie, Geologie und Petrefaktenkunde 2: 51-61.

Canoville, A., de Buffrénil, V. & Laurin, M. 2016: Microanatomical diversity of amniote ribs: an exploratory quantitative study. - Biological Journal of the Linnean Society 118 (4): 706-733.

Clementz, M.T., Holroyd, P.A. & Koch, P.L. 2008: Identifying aquatic habits of herbivorous mammals through stable isotope analysis. - Palaios 23: 574-585.

de Buffrénil, V., Canoville, A., D'Anastasio, R. & Domning, D.P. 2010: Evolution of sirenian pachyosteosclerosis, a model-case for the study of bone structure in aquatic tetrapods. - Journal of Mammalian Evolution 17 (2): 101-120.

Deng, T. 2006: Neogene rhinoceroses of the Linxia Basin (Gansu, China). - Courier-Forschungsinstitut Senckenberg 256: 43-56.

Deng, T. 2008: Comparison between woolly rhino forelimbs from Longdan, Northwestern China and Tologoi, Transbaikalian region. - Quaternary International 179 (1): 196-207.

Deng, T., Wang, X., Fortelius, M., Li, Q., Wang, Y., Tseng, Z.J., Takeuchi, G.T., Saylor, J.E., Säilä, L.K. & Xie, G. 2011: Out of Tibet: Pliocene woolly rhino suggests high-plateau origin of ice age megaherbivores. - Science 333 (6047): 1285.

Diedrich, C.G. 2008: A skeleton of an injured *Coelodonta antiquitatis* from the Late Pleistocene of north-western Germany. - Cranium 25 (1): 29-43.

Flacke, G.L. & Decher, J. 2019: *Choeropsis liberiensis* (Artiodactyla: Hippopotamidae). - Mammalian Species 51 (982): 100-118.

Fortelius, M. 1983: The morphology and paleobiological significance of the horns of *Coelodonta antiquitatis* (Mammalia: Rhinocerotidae). - Journal of Vertebrate Paleontology 3 (2): 125-135.

Fortelius, M., Mazza, P. & Sala, B. 1993: *Stephanorhinus* (Mammalia: Rhinocerotidae) of the western European Pleistocene, with a revision of *S. etruscus* (Falconer, 1868). - Palaeontographia Italica 80: 63-155.

Germain, D. & Laurin, M. 2005: Microanatomy of the radius and lifestyle in amniotes (Vertebrata, Tetrapoda). - Zoologica Scripta 34 (4): 335-350.

Gray, J.E. 1821: On the natural arrangement of vertebrose animals. - London medical repository 15 (1): 296-310.

Gregory, W.K. 1912: Notes on the principles of quadrupedal locomotion and on the mechanism of the limbs in hoofed animals. - Annals of the New York Academy of Sciences 22 (1): 267-294.

Groves, C.P. 1972: *Ceratotherium simum*. - Mammalian Species 8: 1-6.

Groves, C.P. & Kurt, F. 1972: *Dicerorhinus sumatrensis*. - Mammalian Species 21: 1-6.

Groves, C.P. & Leslie, D.M.J. 2011: *Rhinoceros sondaicus* (Perissodactyla: Rhinocerotidae). - Mammalian Species 43 (1): 190-208.

Guérin, C. 1980: Les rhinocéros (Mammalia, Perissodactyla) du Miocène terminal au Pléistocène supérieur en Europe occidentale - Comparaison avec les espèces actuelles. - Documents des Laboratoires de Géologie Lyon 79: 1-1184.

Haeckel, E. 1873: Natürliche Schöpfungsgeschichte. Berlin: Georg Reimer.

Heissig, K. 1972a: Die obermiozäne Fossil-Lagerstätte Sandelzhausen. 5. Rhinocerotidae (Mammalia), Systematik und Ökologie. - Mitteilungen der Bayerischen Staatssammlung für Paläontologie und historische Geologie 12: 57-81.

Heissig, K. 1972b: Paläontologische und geologische Untersuchungen im Tertiär von Pakistan. 5. Rhinocerotidae (Mamm.) aus den unteren und mittleren Siwalik-Schichten. - Abhandlungen Bayerische

Akademie der Wissenschaften, Mathematisch-Naturwissenschaftliche Klasse, Neue Folge 152: 1-112.
Heissig, K. 1999. Family Rhinocerotidae. In: Rössner, G. & Heissig, K., eds.), The Miocene land mammals of Europe, 175-188. München: Verlag Dr. Friedrich Pfeil.
Hoffmann, R., Schultz, J.A., Schellhorn, R., Rybacki, E., Keupp, H., Gerden, S.R., Lemanis, R. & Zachow, S. 2014: Non-invasive imaging methods applied to neo- and paleo-ontological cephalopod research. - Biogeosciences 11 (10): 2721-2739.
Houssaye, A. & Bardet, N. 2012: Rib and vertebral micro-anatomical characteristics of hydropelvic mosasauroids. - Lethaia 45 (2): 200-209.
Houssaye, A. & Botton-Divet, L. 2018: From land to water: evolutionary changes in long bone microanatomy of otters (Mammalia: Mustelidae). - Biological Journal of the Linnean Society 125 (2): 240-249.
Houssaye, A., Waskow, K., Hayashi, S., Cornette, R., Lee, A.H. & Hutchinson, J.R. 2016: Biomechanical evolution of solid bones in large animals: a microanatomical investigation. - Biological Journal of the Linnean Society 117 (2): 350-371.
Kahlke, R.-D. & Lacombat, F. 2008: The earliest immigration of woolly rhinoceros (*Coelodonta tologoijensis*, Rhinocerotidae, Mammalia) into Europe and its adaptive evolution in Palaearctic cold stage mammal faunas. - Quaternary Science Reviews 27 (21): 1951-1961.
Koenigswald, W.v. 2007. 29. Mammalian faunas from the interglacial periods in Central Europe and their stratigraphic correlation. In: Sirocko, F., Claussen, M., Sánchez Goñi, M. F. & Litt, T., eds.), Developments in Quaternary Sciences, 445-454. Amsterdam: Elsevier.
Kriloff, A., Germain, D., Canoville, A., Vincent, P., Sache, M. & Laurin, M. 2008: Evolution of bone microanatomy of the tetrapod tibia and its use in palaeobiological inference. - Journal of Evolutionary Biology 21 (3): 807-826.
Kurtén, B. 1968: Pleistocene mammals of Europe. London: Weidenfeld and Nicolson.
Lartet, E. 1851: Notice sur la colline de Sansan, suivie d'une récapitulation des diverses espèces d'animaux vertébrés fossiles, trouvés soit à Sansan, soit dans d'autres gisements du terrain tertiaire du miocène dans le bassin sous-pyrénéen. Auch: JA Portes.
Laurie, W.A., Lang, E.M. & Groves, C.P. 1983: *Rhinoceros unicornis*. - Mammalian Species 211: 1-6.
Laurin, M., Canoville, A. & Germain, D. 2011: Bone microanatomy and lifestyle: a descriptive approach. - Comptes Rendus Palevol 10 (5): 381-402.
Linnaeus, C. 1758: Systema naturae. Tomus I. Editio decima, reformata. Stockholm: Laurentius Salvius.
Marsh, O.C. 1886: Dinocerata - a monograph of an extinct order of gigantic mammals. - Monograph United States Geological Survey 10: 1-243.
Mihlbachler, M.C. 2005: Linking sexual dimorphism and sociality in rhinoceroses: insights from *Teleoceras proterum* and *Aphelops malacorhinus* from the late Miocene of Florida. - Bulletin of the Florida Museum of Natural History 45 (4): 495-520.
Morton, S.G. 1849: Additional observations on a new species of hippopotamus of Western Africa (*Hippopotamus liberiensis*). - Journal of the Academy of Natural Sciences of Philadelphia, 2nd Series 1: 2-11.
Nakajima, Y. & Endo, H. 2013: Comparative humeral microanatomy of terrestrial, semiaquatic, and aquatic carnivorans using micro-focus CT scan. - Mammal Study 38 (1): 1-8.
NAV 2017: Nomina anatomica veterinaria. Hanover (Germany), Ghent (Belgium), Columbia, MO (U.S.A.), Rio de Janeiro (Brazil): World Association of Veterinary Anatomists.
Owen-Smith, R.N. 1988: Megaherbivores: the influence of very large body size on ecology. Cambridge: Cambridge University Press.
Owen, R. 1848: Description of teeth and portions of jaws of two extinct anthracotherioid quadrupeds (*Hyopotamus vectianus* and *Hyop. bovinus*) discovered by the Marchioness of Hastings in the Eocene deposits on the N.W. coast of the Isle of Wight: with an attempt to develop Cuvier's idea of the classification of pachyderms by the number of their toes. - Quarterly Journal of the Geological Society of London 4: 103-141.
Prothero, D.R. 1998. Rhinocerotidae. In: Janis, C. M., Scott, K. M. & Jacobs, L. L., eds.), Evolution of tertiary mammals of North America - volume 1: terrestrial carnivores, ungulates, and ungulatelike mammals, 595-605. Cambridge: Cambridge University Press.
Richter, J. 2016: Leave at the height of the party: A critical review of the Middle Paleolithic in Western Central Europe from its beginnings to its rapid decline. - Quaternary International 411: 107-128.
Salvador, R.B., Tütken, T., Tomotani, B.M., Berthold, C. & Rasser, M.W. 2018: Paleoecological and isotopic analysis of fossil continental mollusks of Sandelzhausen (Miocene, Germany). - PalZ 92 (3): 395-409.
Sander, P.M. & Andrássy, P. 2006: Lines of arrested growth and long bone histology in Pleistocene large mammals from Germany: what do they tell us about dinosaur physiology? - Palaeontographica, Abt. A 277 (1-6): 143-159.
Sander, P.M., Christian, A., Clauss, M., Fechner, R., Gee, C.T., Griebeler, E.-M., Gunga, H.-C., Hummel, J., Mallison, H., Perry, S.F., Preuschoft, H., Rauhut, O.W.M., Remes, K., Tütken, T., Wings, O. & Witzel, U. 2011: Biology of the sauropod dinosaurs: the evolution of gigantism. - Biological Reviews 86 (1): 117-155.
Schellhorn, R. 2009: Eine Methode zur Bestimmung fossiler Habitate mittels Huftierlangknochen. Doctoral Thesis, Eberhard Karls Universität Tübingen, Tübingen, Germany. http://nbn-resolving.de/urn:nbn:de:bsz:21-opus-39180
Schellhorn, R. 2018a: Mediportal rhinoceroses from the Miocene Sandelzhausen locality (Germany). - Journal of Vertebrate Paleontology, Program and Abstracts 2018: 211.
Schellhorn, R. 2018b: A potential link between lateral semicircular canal orientation, head posture, and dietary habits in extant rhinos (Perissodactyla, Rhinocerotidae). - Journal of Morphology 279 (1): 50-61.
Schellhorn, R. 2019: Inner ear orientation reflects head posture in the woolly rhino (Perissodactyla: Rhinocerotidae). - Journal of Vertebrate Paleontology, Program and Abstracts 2019: 188.
Schellhorn, R. & Pfretzschner, H.-U. 2014: Biometric study of ruminant carpal bones and implications for phylogenetic relationships. - Zoomorphology 133 (2): 139-149.
Schellhorn, R. & Pfretzschner, H.-U. 2015: Analyzing ungulate long bones as a tool for habitat reconstruction. - Mammal Research 60 (2): 195-205.
Schellhorn, R. & Sanmugaraja, M. 2015: Habitat adaptations in the felid forearm. - Paläontologische Zeitschrift 89 (2): 261-269.

Schlösser, M. 2012. Wadersloh – ein bedeutender Fundplatz der spätmittelpaläolithischen Keilmessergruppen. In: LWL-Archäologie für Westfalen und der Altertumskommission für Westfalen (ed.). Archäologie in Westfalen-Lippe 2011, 20-24. Langenweißbach: Beier & Beran.

Schlösser, M. 2013a. Wadersloh - ein Lagerplatz der späten Neandertaler. In: Baales, M., Pollmann, H.-O. & Stapel, B., eds.), Westfalen in der Alt- und Mittelsteinzeit, 64-65. Münster: LWL-Archäologie für Westfalen.

Schlösser, M. 2013b. Werk- und Lagerplätze der Neandertaler im Ur-Lippe-Tal bei Lippstadt. In: Baales, M., Pollmann, H.-O. & Stapel, B., eds.), Westfalen in der Alt- und Mittelsteinzeit, 62-63. Münster: LWL-Archäologie für Westfalen.

Schneider, C.A., Rasband, W.S. & Eliceiri, K.W. 2012: NIH Image to ImageJ: 25 years of image analysis. - Nature Methods 9 (7): 671-675.

Siegfried, P. 1983: Fossilien Westfalens: eiszeitliche Säugetiere - eine Osteologie pleistozäner Großsäuger. - Münstersche Forschungen zur Geologie und Paläontologie 60: 1-163.

Sisson, S. 1914: The anatomy of the domestic animals. Philadelphia and London: W. B. Saunders Company.

Tütken, T. & Vennemann, T. 2009: Stable isotope ecology of Miocene large mammals from Sandelzhausen, southern Germany. - Paläontologische Zeitschrift 83 (1): 207-226.

Wall, W.P. 1983: The correlation between high limb-bone density and aquatic habits in recent mammals. - Journal of Paleontology 57 (2): 197-207.

Wang, B. & Secord, R. 2020: Paleoecology of *Aphelops* and *Teleoceras* (Rhinocerotidae) through an interval of changing climate and vegetation in the Neogene of the Great Plains, central United States. - Palaeogeography, Palaeoclimatology, Palaeoecology 542: 109411.

Wang, K.-M. 1928: Die obermiozänen Rhinocerotiden von Bayern. - Paläontologische Zeitschrift 10 (2): 184-212.

Wood 2nd, H.E. 1937: Perissodactyl suborders. - Journal of Mammalogy 18 (1): 106-106.

Yalden, D.W. 1971: The functional morphology of the carpus in ungulate mammals. - Acta Anatomica 78 (4): 461-487.

Zeuner, F.E. 1934: Die Beziehungen zwischen Schädelform und Lebensweise bei den rezenten und fossilen Nashörnern. - Berichte der Naturforschenden Gesellschaft zu Freiburg i. Br. 34: 21-80.

Zeuner, F.E. 1945: New reconstructions of the woolly rhinoceros and Merck's rhinoceros. - Proceedings of the Linnean Society of London 156 (3): 183-195.

Plate I

Left radius (**A-F**) and radiale (**G-J**) of *Coelodonta antiquitatis* (WMNM P75078) from Wadersloh. Radius in A cranial, B lateral, C caudal, D medial, E proximal, and F distal view. Radiale in G dorsal, H distal, I palmar, and J proximal view. Scale bar 5cm.


A
B
C
D
E
F
G
H
I
J

Plate II

Left carpale 3 (**A-E**) and carpale 4 (**F-J**) of *Coelodonta antiquitatis* (WMNM P75078) from Wadersloh. Carpale 3 in A medial, B dorsal, C lateral, D distal, and E proximal view. Carpale 4 in F medial, G dorsal, H lateral, I distal, and J proximal view. Scale bar 5cm.


A
B
C
D
E
F
G
H
I
J

Plate III

Left metacarpale II (**A-F**) and metacarpale III (**G-L**) of *Coelodonta antiquitatis* (WMNM P75078) from Wadersloh. Metacarpale II in A dorsal, B lateral, C palmar, D medial, E proximal, and F distal view. Metacarpale III in G proximal, H distal, I dorsal, J lateral, K palmar, and L medial view. Scale bar 5cm.


A
B
C
D
E
F
G
H
I
J
K
L

Plate IV

Left metacarpale IV (**A-F**), proximal phalanx of second digit (**G-L**), and proximal phalanx of third digit (M-R) of *Coelodonta antiquitatis* (WMNM P75078) from Wadersloh. Metacarpale IV in A dorsal, B lateral, C palmar, D medial, E proximal, and F distal view. Phalanx proximalis of anterior digitus II in G medial, H dorsal, I lateral, J palmar, K proximal, and L distal view. Phalanx proximalis of anterior digitus III in M palmar, N medial, O dorsal, P lateral, Q proximal, and R distal view. Scale bar 5cm.